Journal of Materials Chemistry A

Accepted Manuscript

ROYAL SOCIETY OF CHEMISTRY

www.rsc.org/materialsA

Journal Name

ARTICLE

A Facile Route to Enhance the Water Flux of Thin-Film Composite Reverse Osmosis Membrane: Incorporating Thickness-Controlled Graphene Oxide in Highly Porous Support Layer†

Received 00th January 20xx,
Accepted 00th January 20xx

DOI: 10.1039/x0xx00000x

www.rsc.org/

Jaewoo Lee,[a] Jun Hee Jang,[a] Hee-Ro Chae,[a] Sang H. Lee,[a] Chung-Hak Lee,*[a] Pyung-Kyu Park,*[b] Young-June Won[c] and In-Chul Kim[d]

In this study, we demonstrated that a reduction in solely the concentration of the polymer solution for preparation of the support layer effectively enhances the water flux of a thin-film composite (TFC) reverse osmosis (RO) membrane. However, a decrease in the polymer concentration caused the sub-surface structure of the support layer to become too porous, which unavoidably weakened the mechanical strength of the support layer. To overcome the problem, we prepared a highly porous support layer with improved mechanical strength by incorporating graphene oxide (GO) platelets. The thickness of the GO platelets was controlled by adjusting the mechanical energy input per volume of precursor solution. We confirmed that well-exfoliated GO platelets (mean thickness; about 1.5 nm) are more effective in enhancing mechanical properties of the support layer. The TFC RO membrane made of the GO composite support layer had almost 1.6 to 4 times higher water flux with comparable salt rejection compared to both the current upper bounds of the RO membranes prepared by modification of the active layer and the commercial RO membranes.

Introduction

Seawater desalination through advanced water treatment has become more necessary than ever before because the water scarcity problem has been accelerated by climate change and increasing demographic pressure.[1-3] Reverse osmosis (RO) technology has been actively sought to alleviate the problems caused by water deficiency because it consumes relatively low energy compared with other desalination technologies such as thermal desalination.[4] For the technology, however, there is still a need for reducing high operational costs associated with high hydraulic pressure.[5] Therefore, high water permeability is desired in the RO membrane to achieve high water flux under low operating pressure while retaining high salt rejection in order to reduce energy consumption in the RO process.

To obtain an RO membrane of high water permeability, various approaches such as surface modification, the addition of nanomaterial, and molecular layer-by-layer assembly have been taken to improve the active layer of the RO membrane.[6-10] It is not surprising that most of the studies on RO membranes have focused on the active layer with no consideration of the support layer, because both salt rejection and most hydraulic resistance affecting the water permeability have been believed to occur in the active layer. In contrast, the support layer of the RO membrane has been regarded as a peripheral or irrelevant factor to membrane performance, because the role of the support layer has been considered only to enable the active layer to endure high pressure compression. As a result, little work has been carried out on the support layer.

Recently, a few studies have been conducted to investigate the influence of the support layer on the active layer formation or performance of the RO membrane.[11-15] Ghosh et al.[14] demonstrated that a support layer with large and hydrophobic surface pores was desirable to produce a rougher and looser active layer because they could be more suitable for the vigorous diffusion of the m-phenylenediamine (MPD) at the polymerization step, thereby leading to improved water flux of the RO membrane. The support layer with large surface pores can be fabricated by decreasing the concentration of the polymer solution or by adding hydrophilic additives. Those approaches might be unsuitable, however, because the former would inevitably weaken the mechanical strength of the support layer and the latter would increase hydrophilicity of the support layer.

In this study, to overcome the above-mentioned problems, we prepared a highly porous polysulfone (PSf) support layer

[a] School of Chemical and Biological Engineering, Seoul National University, 1 Gwanak-ro, Gwanak-gu, Seoul 151-742, Republic of Korea. E-mail: leech@snu.ac.kr; Fax: +82-2-874-0896; Tel: +82-2-880-7075
[b] Department of Environmental Engineering, Yonsei University, 1 Yonseidae-gil, Wonju, Gangwon-do, 220-710, Republic of Korea. E-mail: pkpark@yonsei.ac.kr; Tel: +82-33-760-2890
[c] Center for Environment, Health and Welfare Research, Korea Institute of Science and Technology, Hwarang-ro 14-gil 5, Seongbuk-gu, Seoul, 136-701, Republic of Korea.
[d] Research Center for Biobased Chemistry, Korea Research Institute of Chemical Technology, P.O. Box 107, Daejeon 305-600, Republic of Korea.
† Electronic Supplementary Information (ESI) available: Contact angle measurement, SEM images, Pore size measurement and SPM images. See DOI: 10.1039/x0xx00000x

with improved mechanical strength by incorporating graphene oxide (GO) platelets possessing a superior intrinsic strength due to the sp^2 carbon bonding network.[16, 17] Since GO can enhance mechanical strength of a polymer/GO nanocomposite even at low GO content,[18-22] undesirable side effects stemming from hydrophilicity of GO could become negligible, while successfully reinforcing mechanical properties of the highly porous support layer. Considering that the reinforcing effect of GO platelets correlates with their dispersibility and interfacial interaction between GO platelets and a polymer matrix,[21, 23] we prepared GO platelets possessing the most desirable characteristics to fabricate a PSf/GO nanocomposite support layer with both mechanical strength and highly porous structure, simultaneously. Thin-film composite (TFC) RO membranes were fabricated using the PSf/GO nanocomposite support layer, and then they were compared with commercial membranes as well as the previously reported membranes in open literature in terms of water flux and salt rejection.

Experimental

Fabrication of support layers with various surface pore sizes

Four types of support layers with different surface pore sizes were prepared by employing polymer concentrations ranging from 10 wt% to 25 wt%. PSf (Solvay Korea, Korea) in the amount corresponding to each concentration was dissolved in 1-methyl-2-pyrrolidinone (NMP, Sigma-Aldrich, USA) by stirring for 12 h at 60 °C. After sonication for 1 h, the polymer solutions were kept for 12 h at 25 °C without stirring until bubbles disappeared in the solution prior to casting. After a polyester non-woven fabric was wetted with solvent, the polymer solution was drawn down on the fabric using a micrometric film applicator (Elcometer 3570, Elcometer). The nascent support layers were then immersed in a water bath for 24 h at room temperature for entire liquid-liquid demixing.

Preparation of thickness-controlled GO platelets

The preparation procedures of precursor GO are similar to those described in a previous study.[19] GO platelets were prepared from natural graphite powders (100 mesh, Alfar Aesar, USA) via a modified Hummers method.[24] First, natural graphite powders, sulfuric acid (H_2SO_4, 95%, DAEJUNG, Korea), and nitric acid (HNO_3, 60%, DC chemical Co. Ltd., Korea) were mixed, and then potassium permanganate ($KMnO_4$, Sigma-Aldrich, USA) was gradually added into the mixture under stirring. After stirring at 35–40 °C for 2 h, de-ionized (DI) water was slowly added into the mixture. The mixture was continually stirred at 100 °C until the dark green color of the mixture turned into light brownish. After the mixture was transferred into an ice bath, DI water and H_2O_2 (DUKSAN, Korea) were slowly added into the mixture with vigorous stirring to remove the excess permanganate.[25] The resultant mixture was washed using 5% HCl aqueous solution to eliminate metal ions followed by DI water several times.[26] The obtained graphite oxide (GtO) particles were added to NMP. To prepare different thickness (or exfoliation) of the GO platelets, the as-prepared GtO solution was sonicated by simply adjusting the mechanical energy input per volume of GtO solution. Using a tip sonicator (Sonic VCX-750, Sonics & Materials, Inc., USA) in an ice water bath for 30 min, 92 kJ was applied to 20, 80, and 240 mL of GtO solutions (4 mg/mL), corresponding to the energy inputs of 4.6, 1.2, and 0.4 kJ/mL, respectively.

Fabrication of highly porous support layer reinforced by thickness-controlled GO

The as-produced GO platelets were incorporated in the highly porous support layer according to the following procedure regardless of their thickness. The polymer solution consisting of 10 wt% of PSf and 90 wt% of NMP including various concentrations of GO platelets (0.5, 1, and 2 mg/mL) was casted to prepare the PSf/GO nanocomposite support layers with the following contents of GO platelets relative to PSf weight: 0.5, 0.9, and 1.8 wt%. The nascent highly porous support layers reinforced by GO platelets were then immersed in a water bath for 24 h at room temperature for entire liquid-liquid demixing. All the support layers had similar thickness regardless of the incorporation of GO platelets (Fig. S1 in Supporting Information).

Fabrication of polyamide active layer by interfacial polymerization

TFC membranes were prepared by forming a polyamide selective layer on top of the as-prepared porous PSf support layer via interfacial polymerization. Briefly, PSf support layers were first immersed in an aqueous solution containing 2 wt% MPD (Woongjin Chemical, Korea) with additives [2 wt% triethylamine (TEA, SAMCHUN, Korea), 4 wt% camphor sulfonic acid (CSA, Aldrich, USA), and 1.5 wt% DMSO (DAEJUNG, Korea)] for 1 min. The MPD soaked support layers were rolled with a rubber roller to remove the excess solution from the membrane surface. The MPD saturated support layers were then immersed in a solution of a 0.1 w/v% trimesoyl chloride (TMC, Aldrich, USA) dissolved in hexane (DUKSAN, Korea) for 1 min. After being cured at 60 °C for 10 min, the fabricated TFC membranes were rinsed carefully and stored in deionized water for 30 min at room temperature prior to testing.

Characterization

The Advanced Rheometric Expansion System (ARES) (Rheometric Scientific ARES, Rheometric Scientific, USA) was used to measure the viscosities of the polymer solutions used in this study. The mean surface pore size of the support layer was estimated on the basis of the correlation between solute separation and solute radius in solute transport based on the log-normal probability function].[27] As a test solute, polyethylene glycol (PEG, MW< 20,000) or polyethylene oxide (PEO, MW> 20,000) was chosen. The surface pore size of the support layer was determined by Stokes radii of the test solute corresponding to its molecular weight, which is 50% rejected by the support layer (Fig. S2 in Supporting Information). The amount of the separated solute was measured by a total

organic carbon analyzer (Sievers 5310, GE, USA). The tensile properties of support layers were measured by a Universal testing machine (Instron, USA). All the specimens were measured at a rate of 1 mm/min using 50 N load cells. Zeta potential measurements of the GO dispersions were carried out using an electrophoretic light scattering spectrometer (ELS-Z2, Ostuka Electronic, Tokyo, Japan) at room temperature. The topology of the active layer surface and the thickness of GO platelets were probed by a Scanning Probe Microscope (SPM) (INNV-BASE, VEECO, USA). The relative atomic concentrations of nitrogen and oxygen in active layers were investigated using X-ray photoelectron spectroscopy (XPS) (Axis-HSI, Kratos Analytical, UK) to compare the extent of cross-linking of polyamide. Micro-images were acquired by a Field Emission Scanning Electron Microscope (FESEM) (AURIGA, Carl Zeiss, Germany). Cross-sectional images of membranes were obtained by fracturing the samples immediately after being immersed in liquid nitrogen to prevent them from being destroyed. A sputter coater (SCD 005, BAL-TEC, Germany) was used to coat all samples with platinum for 100 seconds.

Membrane filtration test

Water flux and salt rejection of the prepared TFC membranes were assessed by a bench scale cross-flow system with a 2000 ppm NaCl solution. The effective membrane area is 24.8 cm^2. The cross-flow rate was fixed at 22.2 cm/s, and the temperature was constant at 25 ± 0.5 °C. The RO system was stabilized only with the NaCl solution for 30 min at an applied pressure of 2410 kPa (24.1 bar), and then operated for 30 min at a constant pressure of 1550 kPa (15.5 bar) to measure water flux ($L/m^2/h$). The water flux was calculated by dividing the volume of the collected permeate for 30 min by membrane area. Observed salt rejection was determined by measuring the difference in the salt concentration of the feed (C_f) and the permeate (C_p) with a conductivity meter using the following equation: salt rejection (%) = 100 × (1- C_p/C_f).

Results and discussion

Preparation of support layers with various surface pore sizes

To verify the influence of the support layer on the performance of the RO membrane in terms of water flux and salt rejection, four types of support layers with distinctive structures and surface pore sizes were fabricated by varying the PSf polymer solution concentration from 10 wt% to 25 wt% in light of the fact that typical PSf polymer concentration used for conventional RO membranes ranges over 15 wt% to 25 wt%.[28] This allowed us to examine the effect of the support layer on the water flux of the RO membrane, maintaining all other properties of the support layer except its surface pore size.

It has been reported that the rate of precipitation during a phase inversion process slows down as the viscosity of the polymer solution increases, resulting in the decrease of the surface pore size.[29, 30] Such explanations from earlier studies were in good agreement with our experimental results from the fabrication of the PSf support layer. With the increase of PSf concentration from 10 wt% to 25 wt%, the viscosity of the polymer solution increased (Fig. 1a), and the mean surface pore size of the support layer decreased substantially from 18.2 to 4.4 nm (Fig. 1b and Fig. S2 in Supporting Information).

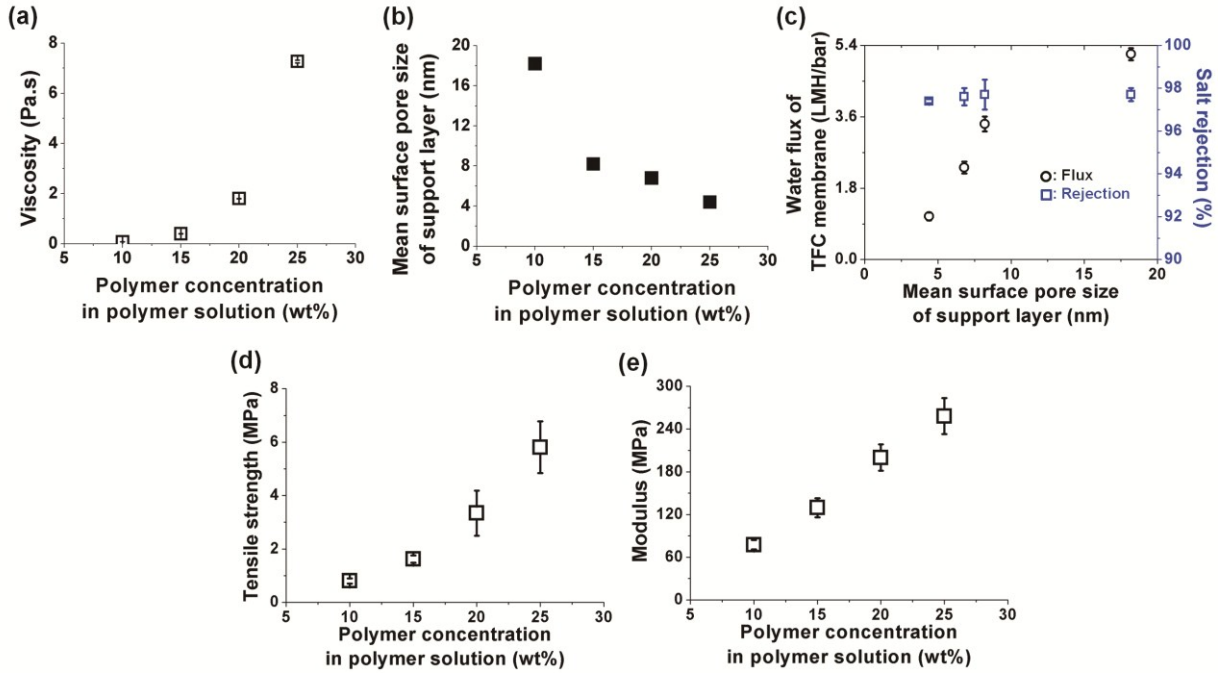

Fig. 1 (a) Viscosities of polymer solution and (b) Mean surface pore size of each support layer as a function of polymer (PSf) concentration. (c) Water flux and salt rejection of RO membranes fabricated using support layers with different mean surface pore sizes. Error bar: standard deviation (n=5). (d) Tensile strength and (e) Young's modulus of support layers as a function of polymer concentration used for the preparation of the support layer. Error bars: standard deviation (n=5).

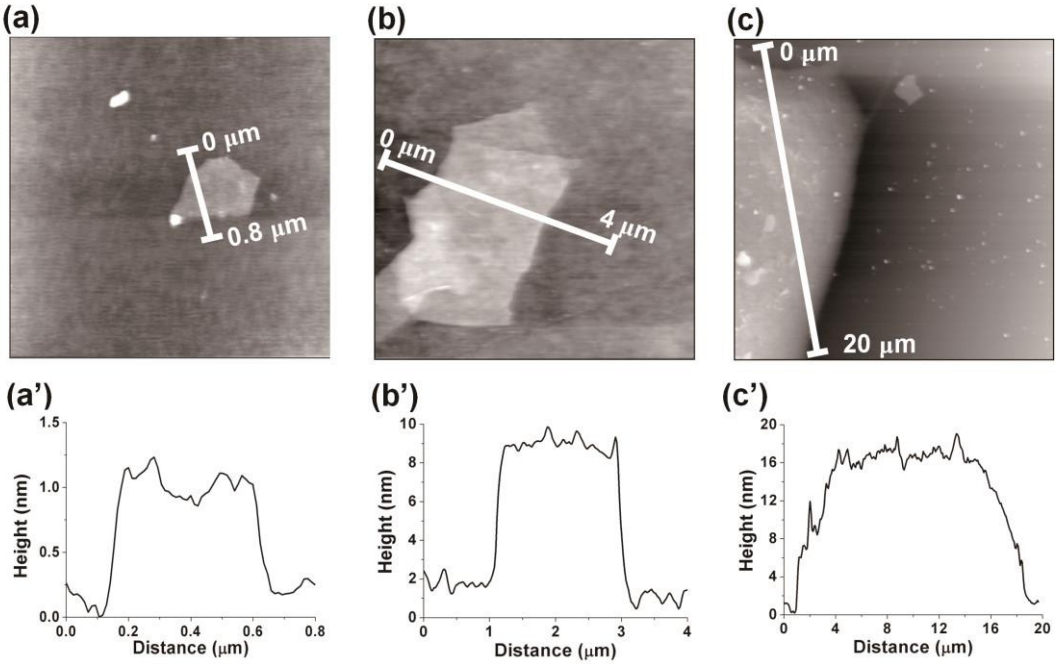

Fig. 2 SPM images of (a) 1-GO, (b) 5-GO and (c) 14-GO on a silicon wafer and the height of each GO platelet along the white line (a', b', c') corresponding to each cross-sectional image.

Influence of the surface pore size of support layer on water flux and salt rejection of the RO membrane

TFC RO membranes were prepared using the as-prepared four types of support layers with different surface pore sizes; the water flux and salt rejection of each TFC membrane were then evaluated. Ghosh et al.[14] reported that a support layer with large and hydrophobic surface pores was desirable to produce a more permeable active layer, and thus to enhance water flux of the RO membrane. In this study, the mean surface pore size of the support layer increased from 4.4 to 18.2 nm with the decrease of PSf concentration (Fig. 1b). Furthermore, because only the PSf concentration was altered, there would not be any significant difference in hydrophobicity between the four types of support layers. Consequently, it was anticipated that the water flux of the as-prepared RO membrane would increase by increasing the mean surface pore size of the support layer. As shown in Fig. 1c, the water flux was clearly augmented from 1.09 (±0.01) to 5.18 (±0.10) LMH/bar with an increase in the surface pore size of the support layer without any significant change in salt rejection.

Preparation of thickness-controlled GO

Although the enhancement of the RO membrane in water flux could be achieved with the decrease of polymer concentration used for the preparation of the support layer, it also had such a negative effect that the sub-surface structure of the support layer became too porous (Fig. S3 in Supporting Information), which in turn provided the support layer with weak mechanical strength (Fig. 1d and 1e). Given that the RO membrane is typically operated under high pressure, it is undesirable to make the RO membrane with such a feeble support layer. Therefore, we devised a new method incorporating GO platelets into the porous support layer, particularly controlling the thickness of the GO platelets to maximize their efficiency.

The GO platelets were made of a graphite oxide (GtO) solution, but the thickness of the GO platelets was dependent on the mechanical energy input per volume of the GtO solution because the energy input affected the extent of exfoliation of the GO platelets. The GO platelets were exfoliated by applying the energy input of 4.6, 1.2, and 0.4 kJ/mL. Successive thickness measurements for five samples of GO platelets prepared at each energy input gave a statistical mean thickness of about 1.5 (±0.4), 5.2 (±0.9), and 14.2 (±1.7) nm, respectively (Fig. 2). Each exfoliation was marked as single-layer (1-GO), five-layer (5-GO), and fourteen-layer GO (14-GO).

Improving mechanical strength of porous support layer with the addition of thickness-controlled GO

Fig. 3a and 3b show the mechanical properties of PSf/GO nanocomposite support layers prepared with 10 wt% of PSf and a different amount of 1-GO or 14-GO. Regardless of the GO content (0.5 wt%–1.8 wt%) and the extent of exfoliation (1- or 14-GO), the tensile strength (Fig. 3a) and modulus (Fig. 3b) of each support layer were augmented compared to those without GO. However, the improvement in the mechanical properties of PSf/GO nanocomposites by GO platelets diminished at the GO content greater than ~1 wt%. This is attributed to the fact that excess GO platelets can provide stress convergence points in the nanocomposites by causing aggregation during phase separation.[19, 31] It is also noteworthy that 1-GO was always more effective than 14-GO in enhancing both mechanical properties. Several studies have ascribed this

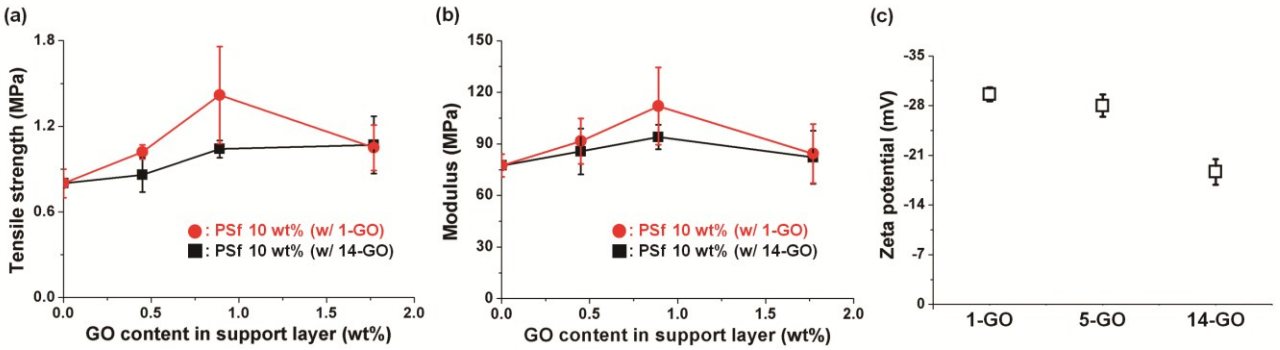

Fig. 3 (a) Tensile strength and (b) Young's modulus of PSf/GO nanocomposite support layers prepared with 10 wt% of PSf and different amount of 14-GO and 1-GO. Error bars: standard deviation (n=5). (c) Zeta potentials of three different groups of GO platelets. Error bars: standard deviation (n=5).

phenomenon to the fact that the load-bearing capability of nanofillers, just like GO platelets, depends on the dispersion and interfacial interaction between the nanofillers and polymer matrix.[32-37] First, the large specific surface area of nanofillers was reported to be the key attribute in relation to the increasing load transfer of the nanofillers.[23] Consequently, more exfoliated 1-GO platelets would be more effective than less exfoliated 14-GO at equivalent loading in the enhancement of mechanical properties. Second, better dispersibility of 1-GO could be another reason. GO platelets are susceptible to agglomeration because of their unusually large specific surface area and additional π-π bonding.[23, 38] However, the agglomeration would have a negative effect on the mechanical strength of the support layer because it would decrease in the specific surface area of platelets and/or formation of stress convergence points (or defects) within the polymer matrix.[19, 21] As shown in Fig. 3c, 1-GO shows the highest zeta potential, which means that 1-GO would have the largest number of exposed oxygenated functional groups at equivalent loading. As a result, 1-GO could maintain more stable dispersion due to strong electrostatic repulsion among them, unlike the insufficiently exfoliated 14-GO.[39]

The support layer with 1-GO of 0.9 wt% gave the highest tensile strength of ~1.42 MPa, which is greater by about 78% than that (~0.80 MPa) without GO. The PSf concentration used for the support layer of a conventional RO membrane ranges over 15 wt%–25 wt%.[28] Taking into account the tensile strength of 1.62 MPa for the support layer prepared with 15 wt% of PSf (Fig. 3a), it was surprising that only with the addition of 0.9 wt% of 1-GO, the tensile strength of the support layer (~1.42 MPa) prepared with such a low PSf concentration (10 wt%) could reach about 90% of that (~1.62 MPa) with 15 wt% of PSf. A similar trend to tensile strength is also observable in Young's modulus (Fig. 3b).

Influence of GO incorporated support layer on the active layer of RO Membrane

Although 1-GO endows a highly porous support layer with excellent mechanical properties, it cannot be a desirable alternative to enhance RO membrane performance if it adversely affects the formation of the active layer with favorable structure for water permeation during the interfacial polymerization. For this reason, we prepared a 10 wt% PSf support layer incorporated with 0.9 wt% 1-GO, and then fabricated the TFC RO membrane (TFC-1-GO) using that support layer. Then, we investigated the influence of GO incorporation on the active layer of TFC-1-GO in terms of surface roughness, cross-linking degree, and thickness of the active layer.

First, the addition of 1-GO into the PSf 10 wt% support layer did not cause any significant change in the roughness of the active layer (Fig. 4a and Fig. S4 in Supporting Information). The average roughness (Ra) of the active layer of the TFC-1-GO membrane was 46.2 (±5.6) nm, while that of the TFC membrane made with a PSf 10 wt% support layer (TFC-10

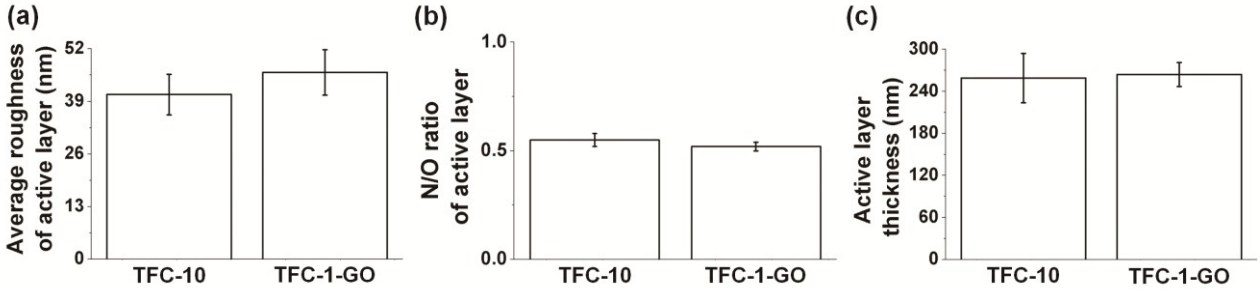

Fig. 4 (a) Average roughness of active layers formed on PSf 10 wt% support layer (left, TFC-10) and PSf 10 wt% support layer reinforced with 0.9 wt% 1-GO (right, TFC-1-GO). Error bar: standard deviation (n=5). (b) Nitrogen/oxygen (N/O) ratio in the active layer of TFC membranes made with PSf 10 wt% support layer (TFC-10) and PSf 10 wt% support layer reinforced with 0.9 wt% 1-GO (TFC-1-GO). Error bar: standard deviation (n=3). Note that the N/O ratio reflects relative cross-linking degree of the active layer. (c) Average thickness of the TFC-10 and TFC-1-GO membranes (scale bar: 1 μm). Error bar: standard deviation of the mean (n=3).

membrane) was 40.7 (±5.0) nm. Second, it is known that there is a positive correlation between the nitrogen/oxygen (N/O) ratio and the cross-linking degree of polyamide active layer.[40] The cross-linking degree of the active layer was examined by the N/O ratios of polyamide active layers in the TFC-10 and TFC-1-GO membranes. However, there was no significant difference in the N/O ratios between the TFC-1-GO membrane [0.52 (±0.02)] and the TFC-10 membrane [0.55 (±0.03)] (Fig. 4b). Third, we also confirmed that the addition of 1-GO into the PSf 10 wt% support layer did not cause any significant change in the active layer thickness. As shown in Fig. 4c and Fig. S5 in Supporting Information, the active layer thickness of the TFC-1-GO membranes was 264 (±17) nm, while that of the TFC-10 was 259 (±35) nm.

These results can be attributed to the fact that the content of GO added in polymer solution in our study was about 160 times lower than the amount of hydrophilic additives used in the quoted reference.[14] Actually, we confirmed that the increase in hydrophilicity of support layer induced by GO platelets was not significant to affect the formation of active layer during the interfacial polymerization by examining the solid-liquid interfacial free energy (Table S1 in supporting information). From these results, we have concluded that the incorporation of 1-GO into the support layer does not cause any significant change in the structure of the TFC RO membrane, but significantly reinforces its mechanical strength, such as its tensile strength and modulus.

Table 1. Comparison of performance of TFC-1-GO membrane with others. Number in parentheses: standard deviation (n=5).

Membrane	Unit water flux [LMH/bar]	Rejection [%]	References
TFC-1-GO	**5.42 (± 0.28)**	**98.2 (±0.7)**	**This work**
mLbL	1.34	98.7	Gu[7]
CNT composite 1	3.41	98.5	Lee[41]
CNT composite 2	2.86	95.7	Kim[42]
Dow-filmte SW30HR	1.93 (±0.08)	99.0 (±0.1)	Tested in this work
Hydranautics LFC-1	2.72 (±0.06)	98.4 (±0.2)	Tested in this work
Hydranautics SWC5	1.56 (±0.03)	97.9 (±0.1)	Tested in this work
Nano H2O SW400ES	2.67 (±0.03)	99.0 (±0.1)	Tested in this work
Woongjin FE	2.94 (±0.04)	98.9 (±0.0)	Tested in this work

Comparison of water flux and salt rejection between TFC-1-GO membrane and other RO membranes

We compared the TFC-1-GO membrane with other various RO membranes in terms of water flux and salt rejection to verify the validity of maximizing the surface pore size of the support layer by reducing the PSf concentration to enhance water flux. For the comparison, we selected three RO membranes reported in literature (two for CNT composites and one for molecular layer-by-layer).[7, 41, 42] We also evaluated the performance of five commercial RO membranes for comparison with the TFC-1-GO membrane for the purpose of examining its potential for industrial applications.

Table 1 reveals that water flux of the TFC-1-GO membrane went as far as to surpass the reported literature values for CNT composite RO membranes or a molecular layer-by-layer RO membrane. In addition, the TFC-1-GO exhibited better membrane performance than diverse commercial RO membranes with comparable salt rejection. These results suggest that a GO-reinforced highly porous support layer enables hand-made RO membranes to outperform commercial membranes.

Mitigation of RO membrane compaction by single-layer GO

Lastly, we conducted the long-term operation of the RO membranes prepared using the 15 wt% support layer, the 10 wt% support layers with and without 0.9 wt% 1-GO to evaluate how effective the GO platelets are in reducing compaction and flux decline of RO membranes caused by high pressure compression.

It has been known that the compaction of the porous support layer can cause a decrease in water flux and an

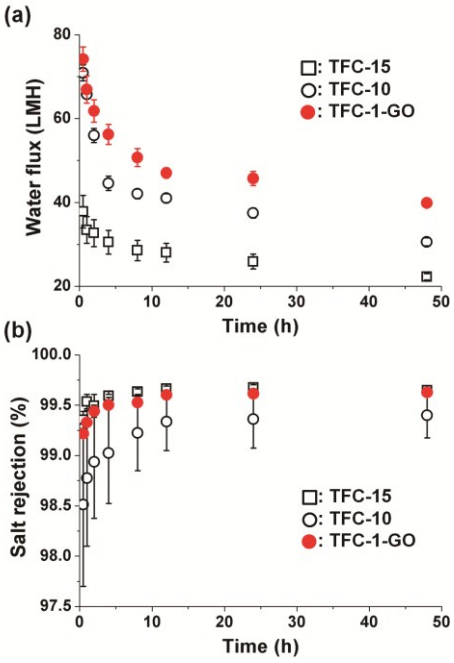

Fig. 5 (a) Water flux and (b) salt rejection of the RO membranes prepared using the 15 wt% support layer (TFC-15), the 10 wt% support layer without and with 0.9 wt% 1-GO (TFC-10 and TFC-1-GO, respectively). Error bar: standard deviation (n=2).

increase in salt rejection of RO membranes because the surface pore radii of support layer become smaller as the porous support layer compacts, thereby increasing the effective path length for the diffusion of water and salt.[43]

The flux decline of RO membranes was observed in our study similarly as described in the early studies. In detail, the water flux of TFC-15 and TFC-1-GO membranes decreased by 41% and 46%, respectively, whereas that of TFC-10 membrane declined by 57% after 48 h (Fig. 5a). This implies that GO platelets enhanced the mechanical stability of 10 wt% support layer to be able to endure the compaction at a level comparable to the 15 wt% support layer.

It is also noteworthy that the increase in salt rejection of TFC-15 and TFC-1-GO membranes (0.29% and 0.41%, respectively) was significantly lower than that of TFC 10 membrane (0.89%). This also supports that TFC-15 and TFC-1-GO membranes experienced less compaction compared to TFC-10 membrane.

Conclusions

Graphene oxide (GO) nanoplatelets were incorporated into a highly porous support layer to fabricate high performance thin-film composite (TFC) reverse osmosis (RO) membrane with both good mechanical strength and high flux. The following conclusion can be drawn:

1) Single-layer GO (1-GO) platelets were more desirable to improve the mechanical strength of polysulfone (PSf) support layer with highly porous structure.

2) 1-GO platelets could be produced by adjusting mechanical energy input per volume of precursor solution.

3) The mechanical strength of the support layer prepared with 10 wt% of PSf and 0.9 wt% 1-GO were comparable to those of the support layer of conventional RO membrane.

4) The GO composite support layer provided TFC RO membrane with 1.6 to 4 times higher water flux with comparable salt rejection compared to both commercial RO membranes and current upper bounds of RO membranes prepared by the modification of active layer.

Acknowledgements

This work was supported by an NRF (National Research Foundation of Korea) grant funded by the Korean Government (MEST, NRF-2010-C1AAA001-0029061) and by Korea Ministry of Environment as ‘‘The Eco-Innovation project (Global Top project) (No. GT-SWS-11-02-007-6)”.

Notes and references

1. S. Piao, P. Ciais, Y. Huang, Z. Shen, S. Peng, J. Li, L. Zhou, H. Liu, Y. Ma and Y. Ding, *Nature*, 2010, **467**, 43-51.
2. T. Oki and S. Kanae, *Science*, 2006, **313**, 1068-1072.
3. T. R. Green, M. Taniguchi, H. Kooi, J. J. Gurdak, D. M. Allen, K. M. Hiscock, H. Treidel and A. Aureli, *Journal of Hydrology*, 2011.
4. M. Elimelech and W. A. Phillip, *Science*, 2011, **333**, 712-717.
5. S. Sourirajan, *Reverse osmosis*, London, UK: Logos Press Ltd., 1970.
6. H.-R. Chae, J. Lee, C.-H. Lee, I.-C. Kim and P.-K. Park, *J. Membr. Sci.*, 2015, **483**, 128-135.
7. J. E. Gu, S. Lee, C. M. Stafford, J. S. Lee, W. Choi, B. Y. Kim, K. Y. Baek, E. P. Chan, J. Y. Chung and J. Bang, *Adv. Mater.*, 2013.
8. M. M. Pendergast and E. M. Hoek, *Energy & Environmental Science*, 2011, **4**, 1946-1971.
9. K. P. Lee, T. C. Arnot and D. Mattia, *J. Membr. Sci.*, 2011, **370**, 1-22.
10. M. Hu and B. Mi, *Environ. Sci. Technol.*, 2013, **47**, 3715-3723.
11. G. Z. Ramon, M. C. Wong and E. Hoek, *J. Membr. Sci.*, 2012, **415**, 298-305.
12. H. I. Kim and S. S. Kim, *J. Membr. Sci.*, 2006, **286**, 193-201.
13. P. S. Singh, S. Joshi, J. Trivedi, C. Devmurari, A. P. Rao and P. Ghosh, *J. Membr. Sci.*, 2006, **278**, 19-25.
14. A. K. Ghosh and E. Hoek, *J. Membr. Sci.*, 2009, **336**, 140-148.
15. N. Misdan, W. Lau, A. Ismail and T. Matsuura, *Desalination*, 2013, **329**, 9-18.
16. M. A. Rafiee, J. Rafiee, Z. Wang, H. Song, Z.-Z. Yu and N. Koratkar, *ACS nano*, 2009, **3**, 3884-3890.
17. C. Lee, X. Wei, J. W. Kysar and J. Hone, *Science*, 2008, **321**, 385-388.
18. J. Zhang, Z. Xu, W. Mai, C. Min, B. Zhou, M. Shan, Y. Li, C. Yang, Z. Wang and X. Qian, *Journal of Materials Chemistry A*, 2013, **1**, 3101-3111.
19. J. Lee, H.-R. Chae, Y. J. Won, K. Lee, C.-H. Lee, H. H. Lee, I.-C. Kim and J.-m. Lee, *J. Membr. Sci.*, 2013.
20. S. Stankovich, D. A. Dikin, G. H. B. Dommett, K. M. Kohlhaas, E. J. Zimney, E. A. Stach, R. D. Piner, S. B. T. Nguyen and R. S. Ruoff, *Nature*, 2006, **442**, 282-286.
21. J. R. Potts, D. R. Dreyer, C. W. Bielawski and R. S. Ruoff, *Polymer*, 2011, **52**, 5-25.
22. M. Ionita, A. M. Pandele, L. Crica and L. Pilan, *Composites Part B: Engineering*, 2014, **59**, 133-139.
23. S. Chatterjee, F. Nafezarefi, N. Tai, L. Schlagenhauf, F. Nüesch and B. Chu, *Carbon*, 2012, **50**, 5380-5386.
24. W. S. Hummers Jr and R. E. Offeman, *J. Am. Chem. Soc.*, 1958, **80**, 1339-1339.
25. G. Zhao, J. Li, X. Ren, C. Chen and X. Wang, *Environ. Sci. Technol.*, 2011, **45**, 10454-10462.
26. C. Wang, C. Feng, Y. Gao, X. Ma, Q. Wu and Z. Wang, *Chemical Engineering Journal*, 2011, **173**, 92-97.
27. S. Singh, K. Khulbe, T. Matsuura and P. Ramamurthy, *J. Membr. Sci.*, 1998, **142**, 111-127.
28. N. Y. Yip, A. Tiraferri, W. A. Phillip, J. D. Schiffman and M. Elimelech, *Environ. Sci. Technol.*, 2010, **44**, 3812-3818.
29. M. Mulder, *Basic Principles of Membrane Technology Second Edition*, Kluwer Academic Pub, 1996.
30. M. J. Han and S. T. Nam, *J. Membr. Sci.*, 2002, **202**, 55-61.
31. Y. Xu, W. Hong, H. Bai, C. Li and G. Shi, *Carbon*, 2009, **47**, 3538-3543.
32. C. Lv, Q. Xue, D. Xia, M. Ma, J. Xie and H. Chen, *The Journal of Physical Chemistry C*, 2010, **114**, 6588-6594.
33. T. Ramanathan, A. Abdala, S. Stankovich, D. Dikin, M. Herrera-Alonso, R. Piner, D. Adamson, H. Schniepp, X.

Chen and R. Ruoff, *Nature nanotechnology*, 2008, **3**, 327-331.

34. B. Das, K. E. Prasad, U. Ramamurty and C. Rao, *Nanotechnology*, 2009, **20**, 125705.
35. A. Yu, P. Ramesh, M. E. Itkis, E. Bekyarova and R. C. Haddon, *The Journal of Physical Chemistry C*, 2007, **111**, 7565-7569.
36. M. Fang, K. Wang, H. Lu, Y. Yang and S. Nutt, *Journal of Materials Chemistry*, 2009, **19**, 7098-7105.
37. D. Cai and M. Song, *Nanotechnology*, 2009, **20**, 315708.
38. F. Gojny, M. Wichmann, U. Köpke, B. Fiedler and K. Schulte, *Composites Sci. Technol.*, 2004, **64**, 2363-2371.
39. X. Lin, X. Shen, Q. Zheng, N. Yousefi, L. Ye, Y.-W. Mai and J.-K. Kim, *ACS nano*, 2012, **6**, 10708-10719.
40. S. H. Kim, S.-Y. Kwak and T. Suzuki, *Environmental science & technology*, 2005, **39**, 1764-1770.
41. H. D. Lee, H. W. Kim, Y. H. Cho and H. B. Park, *Small*, 2014, **10**, 2653-2660.
42. H. J. Kim, K. Choi, Y. Baek, D.-G. Kim, J. Shim, J. Yoon and J.-C. Lee, *ACS applied materials & interfaces*, 2014, **6**, 2819-2829.
43. M. T. M. Pendergast, J. M. Nygaard, A. K. Ghosh and E. M. Hoek, *Desalination*, 2010, **261**, 255-263.

TOC ART

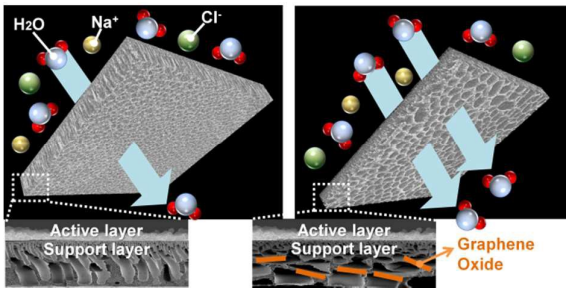

Incorporation of single-layer graphene oxide in highly porous support layer provides thin-film composite reverse osmosis membrane with superior water flux, retaining high salt rejection.